Chemical Engineering Journal 113 (2005) 145–152

Chemical Engineering Journal

www.elsevier.com/locate/cej

Hydrodynamic characterization of a trickle bed air biofilter

Gloria Trejo-Aguilar, Sergio Revah, Ricardo Lobo-Oehmichen *

Departamento de Ingeniería de Procesos e Hidráulica, Universidad Autónoma Metropolitana-Iztapalapa, San Rafael Atlixco 186, Del Iztapalapa C.P. 09340, México, DF, Mexico

Received 20 November 2004; received in revised form 27 February 2005; accepted 6 April 2005

Abstract

This paper reports the effect of superficial liquid mass flow rate and bed void fraction on the pressure drop, dynamic liquid hold-up, mean liquid residence time and biofilm wetting, in a co-current down-flow xylene-removing trickle bed air biofilter (TBAB). The gas–liquid pressure drop increased with liquid mass flow rate and it also increased with diminishing bed void fraction, the effect being larger at bed void fraction of 0.41. Dynamic liquid hold-up was higher with increasing liquid mass flow rate, and showed a maximum when the bed void fraction was 0.69. The same pattern was observed for the mean liquid residence time and the wetting efficiency. Liquid residence time distribution curves indicate stagnant regions, channeling, and recirculation within the TBAB, whose effects were larger at a bed void fraction of 0.41. A maximum elimination capacity of 30 g/m^3 h, with 78% removal efficiency, was reached when the bed void fraction was 0.8 and the liquid mass rate 14.1 kg/m^2 s. An average minimum elimination capacity of 6 g/m^3 h was observed at a bed void fraction of 0.41. Xylene isomers were preferentially removed in the order of $o > m > p$.
© 2005 Elsevier B.V. All rights reserved.

Keywords: Trickle bed air biofilter; Bed void fraction; Biofilm wetting; Xylene isomers; Hydrodynamics

1. Introduction

Gaseous pollutant removal efficiencies in a trickle bed air biofilter (TBAB) depend on both physico-chemical and biological phenomena. Hydrodynamic variables, such as the fluid phases' flow regimes, pressure drop, liquid hold-up, bed void fraction, and biofilm wetting, have an impact on the substrates and the oxygen mass transfer rates to the biofilm [1,2], and thus, on the TBAB removal capacity. However, little attention has been given to TBAB hydrodynamic characterization.

In a TBAB, the liquid flow is the main agent for substrate and oxygen transport from the gas to the biofilm. It has been found [3] that there is a strong relationship between liquid flow and the TBAB elimination capacity. However, it is not certain whether the non-wetted parts of a biofilm (biofilm without a liquid film flowing over it) in a TBAB have a considerable biological activity. Partial wetting may cause a limitation in substrate and oxygen supply to the biofilm. To the best of our knowledge, partial wetting has not being quantified in TBAB.

Biofilm wetting depends on a number of variables that characterize the hydrodynamics of a TBAB. Gas and liquid flows, reactor dimensions, the type and size of packing used as a biofilm support, amount of biomass present, bed void fraction, pressure drop, liquid hold-up, and liquid distribution are some of the most important variables and parameters that may affect biofilm wetting. Several of these also have a strong impact on mass transfer coefficients and on the physical characteristics of the biofilm itself. In a TBAB, it may be useful to introduce a parameter to estimate how much of the biofilm surface area is wetted by the descending liquid that causes substrate and oxygen mass transfer to the biofilm. The biofilm is also wetted by stagnant liquid (static hold-up), though this wetting contributes little to liquid–biofilm mass transfer (and thus to bioreaction) because in a stagnant liquid the mass transport mechanism is only molecular diffusion, which in liquids is very slow. We shall call this parameter wetting efficiency (f_w), and it will be defined as the fraction of the total biofilm superficial area that is wetted by flowing

* Corresponding author. Tel.: +52 55 58 04 46 48/49/50/51/52; fax: + 52 55 58 04 49 00.
E-mail address: lobo@xanum.uam.mx (R. Lobo-Oehmichen).

1385-8947/$ – see front matter © 2005 Elsevier B.V. All rights reserved.
doi:10.1016/j.cej.2005.04.001

liquid. For non-biological systems, it has been shown that wetting efficiency depends on pressure drop, liquid hold-up, bed void fraction, and properties of the fluids [4]. Information on the relation between the variables that affect biofilm wetting and on the effect of hydrodynamics on TBAB performance is rather scarce. To date, there are no correlations specifically developed for TBAB that allow the reliable estimation of hydrodynamic parameters.

The purpose of this paper is to investigate the effect of superficial liquid mass flow rate and bed void fraction on pressure drop, dynamic liquid hold-up, total liquid hold-up, mean liquid residence time, and biofilm wetting efficiency, in a co-current down flow TBAB that removes a mixture of xylene isomers as a model pollutant. The TBAB biological response was studied with the xylene elimination capacity, removal efficiency, and isomer biodegradability selectivity.

The relation between the hydrodynamic variables and the TBAB performance is also discussed in the paper.

2. Materials and methods

2.1. Biotrickling filter

Experiments were carried out in an acrylic TBAB (0.15 m i.d. × 1.32 m of total packed length of 316 SS 0.5 in Pall rings with a bed void fraction of 0.95). A schematic diagram of the TBAB system is shown in Fig. 1. The TBAB consists of four 34 cm long identical modules, each supported on a SS grid. Below the three first modules there is a liquid redistribution plate. The TBAB also has five equidistant sampling ports along its height. Xylene-saturated air, mixed with a second airflow, is introduced at the top of the bioreactor, and the flow of both streams was controlled by mass-flow controllers (Aalborg 0-5 and 0-100 LPM, USA). The liquid phase is also fed to the top of the TBAB where it is distributed over the TBAB cross-sectional area by a liquid distributor (a nylon plate with 37 pieces of 316 SS tubing 0.25 in nominal ×1 in length). Gas and liquid contact exist prior to their entrance to the bed. Below the TBAB, there is a 16 L holding tank, from which the liquid is recirculated to the top of the TBAB. The liquid pH was controlled by the addition of 1N HCl by a pH controller (Barnanat, USA). All gas and liquid lines were composed of copper tubing.

2.2. Experimental plan

Four sets of experiments were performed, each corresponding to a specific bed void fraction (ε_B): 0.95, 0.80, 0.69, and 0.41. The first value corresponds to the bed without biomass; the others represent different stages of biomass growth. Bed void fractions of 0.8, 0.69, and 0.41 were reached after 29, 80, and 119 days of operation after start-up, respectively. During each set of experiments, the superficial liquid mass flow rate (L) was varied to observe its effect on the hydrodynamic and biological parameters. The L-values

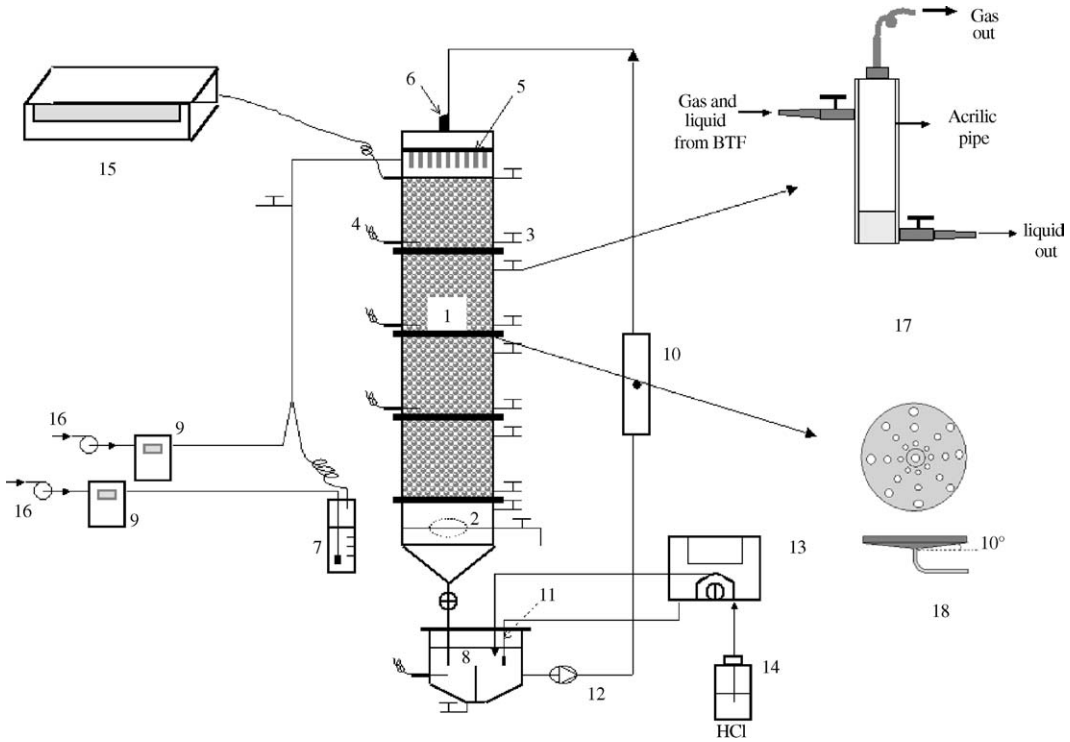

Fig. 1. Schematic diagram of the TBAB system. (1) TBAB, (2) floodgate, (3) sampling ports, (4) thermocouples, (5) liquid distributor, (6) tracer injection port, (7) xylenes saturator, (8) liquid holding tank, (9) mass flow controller, (10) flowmeter, (11) pH electrode, (12) pump, (13) pH controller, (14) HCl solution, (15) automatic temperature acquisition system, (16) air compressor, (17) trap to separate gas and liquid phases, (18) liquid redistributors.

used for each experimental set were 6.2, 8.8, 11.5, and 14.1 kg/m^2 s. The superficial gas mass velocity (G) was kept constant at 4.47×10^{-2} kg/m^2 s for all experiments. These combinations of flows allowed the TBAB to operate in the trickle flow regime, as defined in a flow-regime map prepared by Gianetto and Specchia [5]. The hydrodynamic parameters evaluated were pressure drop, dynamic liquid hold-up, total liquid hold-up, mean liquid residence time and wetting efficiency. For the biological response the following parameters were determined: inlet and outlet concentration of total and individual xylene isomers at each sampling port, total elimination capacity, total xylene and the individual isomer removal efficiencies, and CO_2 production expressed as a mineralization percentage. Calculation of these parameters was accomplished using the following expressions:

$$\mathrm{EC} = \frac{F_G}{V_\mathrm{r}}(C_{G,\mathrm{in}} - C_{G,\mathrm{out}}) \quad (1)$$

$$\%\mathrm{RE} = \frac{C_{G,\mathrm{in}} - C_{G,\mathrm{out}}}{C_{G,\mathrm{in}}} \times 100 \quad (2)$$

$$\%P_{\mathrm{CO}_2} = \mathrm{EC} \times \frac{8M_{\mathrm{CO}_2}}{M_{\mathrm{Xyl}}} \times 100 \quad (3)$$

where $C_{G,\mathrm{in}}$ and $C_{G,\mathrm{out}}$ represent inlet and outlet xylene concentration, respectively (g/m^3); F_G total air flow (m^3/h); V_r reactor volume (m^3); EC elimination capacity (g/m^3 h); %RE removal efficiency (%); $\%P_{\mathrm{CO2}}$ mineralization percentage (%); and M represents molecular weight (g/mol).

Before each run, it was necessary to wait approximately 80 h to ensure that the TBAB was operating at a pseudo-steady state; this was assumed to occur when the changes in the xylene removal efficiency were within 5%. The xylene isomers were fed in equimolar proportions during each set of experiments. Although the inlet load was maintained constant during each experimental set, there were some variations between each set. The inlet loads were 42, 52, and 44 g/m^3 h for the experiments at void fractions of 0.80, 0.69, and 0.41, respectively. All experiments were carried out at 30 °C in a temperature-controlled room. It was observed that temperature along the bed did not change, and thus, the TBAB was considered to be isothermal.

2.3. Microorganisms

A bacterial and fungal consortium obtained from a 260 L biofilter previously operated with gasoline vapors [6] was used. This consortium was acclimated to xylene as their sole carbon and energy source during 1 month before the TBAB inoculation.

2.4. Liquid phase

The liquid phase recirculated through the bed was prepared with a ratio of 9 L distilled water to 1 L of a mineral solution [7] containing KNO_3 as a nitrogen source. The diluted solution was used to limit available nitrogen to control biomass growth, thus ensuring constant bed void fraction during each experimental set. When it was necessary to change the bed from one void fraction to the next, biomass was grown by increasing the available nitrogen using the undiluted mineral solution. Liquid phase pH was adjusted to 6.9 using 1N HCl.

The mineral medium composition was (g/L): KNO_3 4.6; KH_2PO_4, 0.6; K_2HPO_4, 2.4; $MgSO_4{\cdot}7H_2O$, 1.5; $CaSO_4{\cdot}2H_2O$, 0.15; trace elements solution, 5 mL/L. The trace elements solution was (g/L): $FeCl_3{\cdot}6H_2O$, 0.54; $ZnSO_4{\cdot}7H_2O$, 0.144; $MnSO_4{\cdot}H_2O$, 0.84; $CuSO_4{\cdot}5H_2O$, 0.025; $CoCl_2{\cdot}6H_2O$, 0.026; H_3BO_3, 0.00662; $NiCl_2{\cdot}6H_2O$, 0.009; $Na_2MoO_4{\cdot}2H_2O$, 0.049; EDTA, 0.76.

2.5. Analytical methods

The xylene isomers were analyzed by FID/GC (Agilent 6890 N) equipped with a 25 m × 250 μm × 0.20 μm nominal capillary column (AT-TM-WAX, Alltech, USA). Helium was used as a carrier gas at a flow rate of 0.8 mL/min. The GC was supplied with 30 mL/min of hydrogen and 300 mL/min of air. The injector, oven, and detector temperatures were maintained at 200, 65, and 160 °C, respectively. CO_2 was analyzed by TCD gas chromatography (Agilent 6890 N), equipped with a packed column (Porapack Q S.0.0.730-83977-13, USA). Helium was used as a carrier gas at a flow rate of 4.1 mL/min. Injector, oven, and detector temperatures were maintained at 110, 65, and 250 °C. The air samples were collected in a 0.5 L glass bulb (Alltech, USA). Samples of 250 μL of air were taken from this bulb using a precision analytical syringe (VICI Precision Sampling, USA) and injected into both the GC/FID and the GC/TCD injection ports. The xylene isomers retention times (min) were: *p*-xylene, 6.0; *m*-xylene, 6.2; and *o*-xylene, 7.5.

Pressure drop along the bed was measured by a U-tube manometer. The reported values correspond to the difference between the outlet and the inlet pressure. Total liquid hold-up (ε_L) was defined as the bed volume fraction occupied by the flowing and non-flowing liquid phase, and it was obtained by multiplying the volumetric liquid flow rate by the mean liquid residence time. Dynamic liquid hold-up ($\varepsilon_{\mathrm{Ld}}$) was defined as the fraction of bed volume occupied by flowing liquid, and was determined by the drainage method. The latter consists of collecting and measuring the liquid that drains at the bottom of the bed after suspending the liquid. After pseudo-steady state, the liquid feed was suspended to the column, and the liquid in the column was collected for 30 min by closing the floodgate. Static liquid hold-up ($\varepsilon_{\mathrm{Ls}}$) is the bed volume fraction occupied by stagnant liquid, and it was calculated as the difference between total and dynamic liquid hold-up.

Mean liquid residence time was determined by the pulse technique using dextran blue (Sigma Chemical, USA) as a tracer. The technique assumes that the tracer is distributed between both flowing and stagnant liquid. A 10 mL volume of dextran blue solution corresponding to 6000 ppm was

injected at the tracer injection port. Liquid samples (3–5 mL) were collected at the bottom of the bed each second during 60 s. The samples were centrifuged (Eppendorf Digital centrifuge 5415D, USA) at 11,000 rpm for 25 min to separate the biomass. The supernatant liquid was analyzed by a spectrophotometer (ThermoSpectronic Genesys 6, USA) at 650 nm.

The bed void fraction (ε_B) was determined by flooding. The TBAB column was slowly filled up with water allowing for air venting. Then the bed was drained module by module, and the liquid drained was measured. The total volume of water drained from the bed was divided by the total bed volume to give the void fraction.

Wetting efficiency (f_w) was calculated by the model proposed by Pironti et al. [4]. It is defined in terms of pressure drop, total liquid hold-up, and bed void fraction Eq. (4) and compares the product of liquid–solid shear stress with the specific area in the two-phase flow to that of a liquid-filled bed at the same intrinsic liquid and gas velocities. By means of an overall force balance in the liquid and gas phases, it is possible to relate each shear stress with pressure drop, measured at two-phase, liquid-filled and gas-filled operation:

$$f_w = \frac{g[\rho_L\varepsilon_L + \rho_G(\varepsilon_B - \varepsilon_L)] - \varepsilon_B\rho_G g + \varepsilon_B[(\Delta P/L)_{2-phase} - (\Delta P/L)_{gas-filled}]}{\varepsilon_B g(\rho_L - \rho_G) + \varepsilon_B[(\Delta P/L)_{liquid-filled\,bed} - (\Delta P/L)_{gas-filled}]} \quad (4)$$

where ρ_G and ρ_L are the gas and liquid densities, respectively; $(\Delta P/L)_{2\text{-phase}}$ the pressure drop per unit length when both gas and liquid are flowing inside the TBAB; $(\Delta P/L)_{gas\text{-phase}}$ the pressure drop per unit length when only the gas flows; $(\Delta P/L)_{liquid\text{-filled bed}}$ the pressure drop per unit length when the bed is full of flowing liquid; and g the acceleration due to gravity.

3. Results and discussion

3.1. Hydrodynamic characterization

Fig. 2 shows that at the same bed void fraction, gas–liquid pressure drop per unit length increases with the superficial liquid mass flow rate, the effect being more pronounced at high liquid rates. As biomass grows, bed void fraction diminishes, as does the free TBAB cross-sectional area. At constant liquid rate, the pressure drop increases, first slowly (from 0.95 to 0.69 bed void fractions values), and then rapidly (from 0.69 to 0.41 bed void fraction values). The reduction of the available area for fluid flow causes the pressure drop to increase.

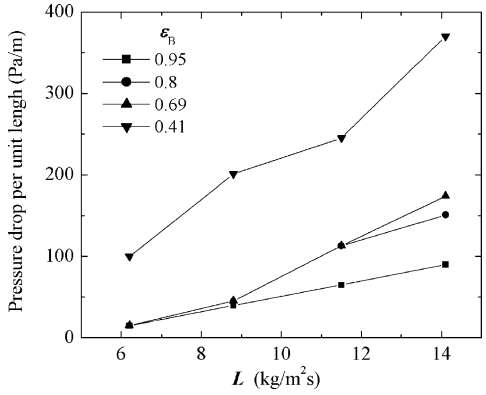

Fig. 2. Effect of superficial liquid mass flow rate (L) on pressure drop at different bed void fractions.

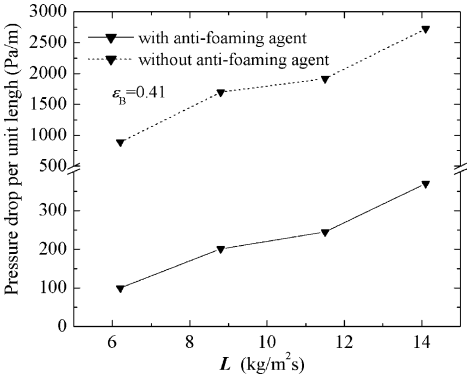

Fig. 3. Effect of the antifoaming agent on pressure drop.

The gas–liquid flow caused a considerable amount of foam inside the TBAB, a large pressure drop, and some TBAB operational difficulties, particularly at the 0.41 bed void fraction. To diminish foam formation, a few drops of an antifoaming agent (Clerol®) were added to the recirculating liquid, causing the pressure drop to fall sharply. This is illustrated in Fig. 3, where pressure drop experiments with and without the antifoaming agent in the recirculating liquid are compared at $\varepsilon_B = 0.41$. The reduction in pressure drop may be attributed to the foam suppression, caused by the antifoaming agent. All experiments reported here were performed with the antifoaming agent, except for those at the 0.95 bed void fraction.

Increasing the liquid flow rate causes the dynamic liquid hold-up to increase, for all bed void fractions, as shown in Fig. 4. This means that with an increase of dynamic

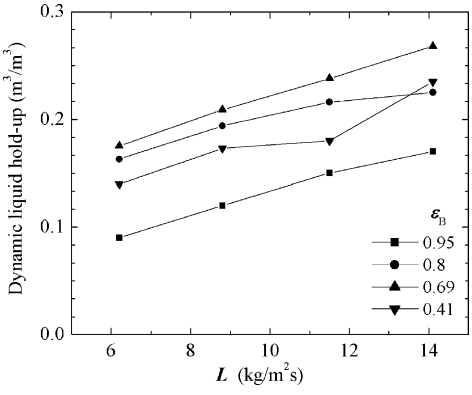

Fig. 4. Effect of superficial liquid mass flow rate (L) on dynamic liquid hold-up at different bed void fractions.

liquid hold-up, the thickness of the flowing liquid film over the biofilm is greater and probably more biofilm is wetted. At bed void fractions above 0.69, the dynamic hold-up always increased with decreasing void fraction. However, on further reduction of the bed void fraction below 0.69, the dynamic hold-up decreased. The increase in the dynamic hold-up with decreasing bed void fraction (down to $\varepsilon_B = 0.69$) may be due to the increasing presence of stagnant regions within the biomass, where liquid is loosely retained; when the liquid flow is suspended to determine the dynamic liquid hold-up, the retained liquid drains and is accounted for as such. However, when the bed void fraction reaches 0.41, there seems to be a qualitative change in the bed structure, where channeling, stagnant regions, and internal recirculation increase. The likelihood of this hypothesis rises when it is seen in the light of the mean liquid residence time and the liquid residence time distribution (RTD) curves behavior, as discussed below.

Fig. 5 shows that at constant bed void fraction, the mean liquid residence time is reduced with increasing liquid flow rate, as expected. It is also apparent that at a constant liquid rate, the mean liquid residence time first increases with diminishing bed void fraction (down to $\varepsilon_B = 0.69$), and then the trend reverses upon further bed void fraction reduction (down to $\varepsilon_B = 0.41$). Fig. 6 shows residence time distribution (RTD) curves for bed void fractions of 0.69 and 0.41. The vertical arrows indicate the mean liquid residence time at each liquid mass flow rate. These curves display: (a) the main portion appears before the mean liquid residence time and the curves have long tails, indicating the existence of stagnant regions within the TBAB; (b) several peaks and "humps", indicating channeling and internal recirculation. In the 0.41 bed void fraction experiments, the curves show a shift toward the left (lower residence times, and thus, lower total liquid hold-up), shorter main peaks, wider spread, and longer tails with respect to the curves for 0.69 bed void fraction. Such behavior is indicative of larger stagnant regions, channeling and internal liquid recirculation for the 0.41 bed void fraction experiments. From the RTD curves shown, it is possible to conclude that the liquid flow pattern in the bioreactor deviates considerably from plug flow and even from dispersed plug flow. More likely the liquid flow pattern would have to be described by the so-called two-region model, where a dynamic region in dispersed plug flow exchanges mass with a stagnant region. Unfortunately, to the best of our knowledge, there are no other published data with which to compare the present results.

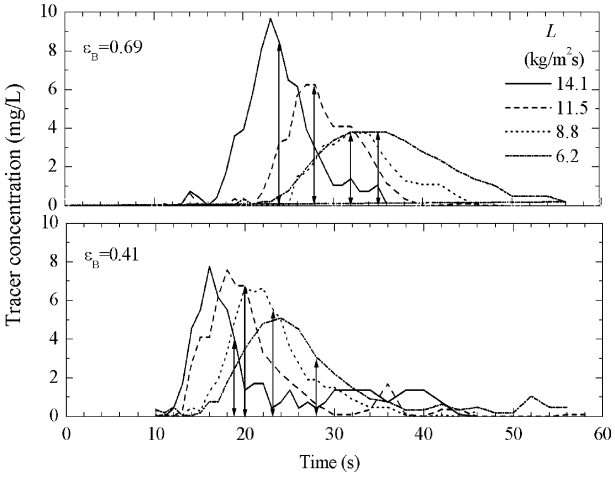

Fig. 6. Liquid residence time distribution curves at different superficial liquid mass flow rates, at bed void fractions of 0.69 and 0.41. The arrows indicate the mean residence time.

Total liquid hold-up increases almost linearly with the liquid flow rate, as shown in Fig. 7. It may be seen that it follows the same pattern as the dynamic liquid hold-up and the mean liquid residence time. At a constant liquid rate, it first increases with diminishing bed void fraction (down to $\varepsilon_B = 0.69$) and then decreases when $\varepsilon_B = 0.41$. Although not shown here, the static liquid hold-up varies from 0.025 to 0.080, and shows a small dependence on the liquid flow, but varies with bed void fraction. Even though it is a complex matter, understanding liquid hold-up in a TBAB is important because not all of the liquid present in the bioreactor contributes to effective wetting. While the static hold-up wets the biofilm, it may be contributing little to liquid–biofilm mass transfer and thus to the TBAB-removal capacity.

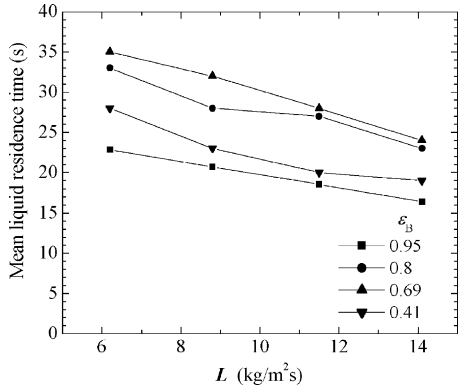

Fig. 5. Effect of superficial liquid mass flow rate (L) on mean liquid residence time at different bed void fractions.

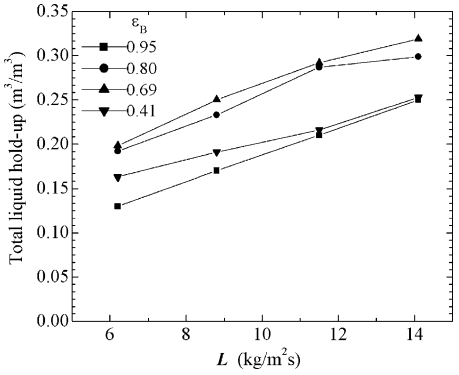

Fig. 7. Effect of superficial liquid mass flow rate (L) on total liquid hold-up at different bed void fractions.

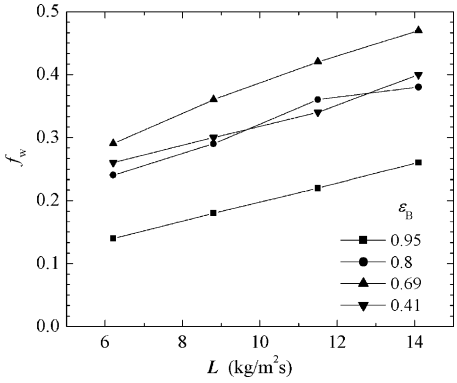

Fig. 8. Effect of superficial liquid mass flow rate (L) on wetting efficiency at different bed void fractions.

Wetting efficiency, Fig. 8, was calculated with Eq. (4) from the gas–liquid (two-phase) pressure drop data shown in Fig. 2, the pressure drop data in Table 1, and the total liquid hold-up data in Fig. 7. Wetting efficiency follows the same trends as those observed for dynamic liquid hold-up and mean liquid residence time. It can be seen that wetting efficiency improves with increased liquid flow rate, as expected. The increase in the wetting efficiency with the reduction of the bed void fraction can be related to the reduction of biofilm superficial area as biomass grows. However, for $\varepsilon_B = 0.41$ wetting efficiency declines, probably due to strong liquid channeling. Since wetting efficiency depends upon pressure drop and liquid hold-up, its estimation using the pressure drop data, obtained without antifoaming agent in the liquid, gives larger values than those calculated from pressure drop and liquid hold-up data with antifoaming agent present. In the absence of antifoaming agent, the values ranged from 24% larger at the lowest liquid rate to 38% at the highest liquid rate when $\varepsilon_B = 0.41$. The Pironti et al. [4] equation, Eq. (4), used to estimate wetting efficiency was developed for solid packing that are evenly distributed in the bed, resulting in a bed void fraction that is also evenly distributed. However, bed void fraction in a TBAB is not distributed in the same manner because biomass does not grow uniformly. Thus, the wetting efficiency estimations reported here are only approximate.

3.2. TBAB performance

Xylene biodegradation in the TBAB was observed three days after start-up. The relationship between the total xylene-elimination capacity and the inlet carbon load showed a maximum elimination capacity of nearly 33 g/m^3 h with 42% of removal efficiency, for a xylene inlet load of around 78 g/m^3 h (Fig. 9). Under these conditions, the critical elimination capacity was approximately 11 g/m^3 h. It is important to note that these results were obtained using a nitrogen-diluted mineral medium as recirculating liquid. Similar results have been obtained with gas–solid biofilters [9,10], where removal efficiencies of nearly 100% were obtained at loads of 15 and 10 g/m^3 h, respectively. It should be recalled that when it was necessary to grow biomass in order to change the bed void fraction, an undiluted mineral solution was used. In this case, the best TBAB performance was EC = 78 g/m^3 h; %RE = 67 and 20 g/m^3 h critical elimination capacity, for an inlet load of 118 g/m^3 h, a bed void fraction of 0.8, and a liquid mass flow rate of 15 kg/m^2 s (Fig. 9). These overall TBAB performance data were obtained at $\varepsilon_B = 0.80$ and $L = 14.1$ kg/m^3 h.

Table 1
Pressure drop data for the gas-filled and liquid-filled bed

ε_B	L (kg/m^2 s) ($\Delta P/L$)$_{\text{liquid-filled bed}}$ (Pa/m)				G (kg/m^2 s) ($\Delta P/L$)$_{\text{gas-filled}}$ (Pa/m)
	14.1	11.5	8.8	6.2	4.47×10^{-2}
0.95	169	143	117	92	15
0.80	287	151	136	87	15
0.69	332	241	181	136	15
0.41	6125	6020	5914	5809	23

Table 2 shows the elimination capacity, removal efficiency, and CO_2 mineralization data. It may be noted that the bed void fraction reduction had a negative effect on the xylene-elimination capacity and removal efficiency. A possible explanation might be that a reduction of the biofilm surface area occurs when biomass grows, and thereby, reducing bed void fraction. Also, at the lowest bed void fraction, the wetting efficiency diminishes and less substrate is transported to the biofilm.

At a bed void fraction of 0.8, increasing the liquid mass flow rate had a positive influence on elimination capacity and removal efficiency, and could have been directly related to wetting efficiency. However, on further bed void fraction reduction ($\varepsilon_B = 0.69$), the liquid mass flow rate had no effect on the elimination capacity, and apparently the latter was insensitive to wetting efficiency, although this last parameter increased with liquid flow rate. At the lowest bed void fraction of 0.41, the elimination capacity was greatly reduced, and was still insensitive to liquid mass flow rate and to wetting efficiency. It appears that in the present system the liquid mass flow rate had an effect on elimination capacity only when the bed void fraction was 0.8.

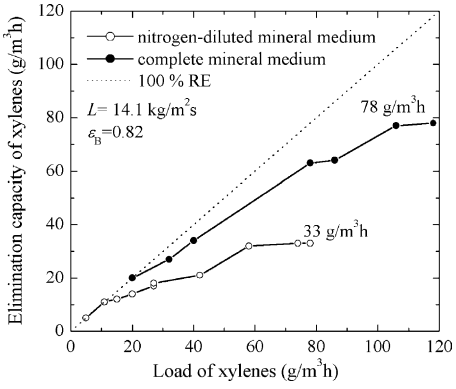

Fig. 9. Elimination capacity as a function xylene inlet load for experiments with complete mineral medium and with mineral medium with limited nitrogen.

Table 2
TBAB total xylene elimination capacity, removal efficiency and mineralization, using a nitrogen-limited recirculating liquid

ε_B	Load (g/m^3 h)	L (kg/m^2 s)											
		Elimination capacity (g/m^3 h)				Removal efficiency (%)				Mineralization (%)			
		14.1	11.5	8.8	6.2	14.1	11.5	8.8	6.2	14.1	11.5	8.8	6.2
0.80	42	30	29	22	20	78	70	50	48	nd	nd	nd	nd
0.69	52	28	28	27	29	54	53	53	56				
0.41	44	8	5	5	6	18	11	12	13	$\overline{58}$	$\overline{57}$	$\overline{50}$	$\overline{41}$

nd: not determined. Overbar on numbers: average value.

Table 3
TBAB individual removal of xylene isomers[a] using a nitrogen-diluted recirculating liquid

ε_B	L (kg/m^2 s)											
	o-Xylene (%)				*m*-Xylene (%)				*p*-Xylene (%)			
	14.1	11.5	8.8	6.2	14.1	11.5	8.8	6.2	14.1	11.5	8.8	6.2
0.80	83	78	57	49	81	73	59	50	65	57	43	45
0.69	63	62	60	63	55	55	54	56	46	44	45	50
0.41	15	13	13	12	10	11	11	15	11	11	12	13

[a] Calculated with respect to the amount of each isomer in the feed.

Since no xylene was detected in the liquid phase, it may be assumed that mass transfer at the gas–liquid interface controlled the TBAB rate of xylene removal [1]. The low solubility of xylene suggests that the main mass transfer resistance was located in the liquid. It was unexpected that the elimination capacity showed a low sensitivity with respect to liquid mass flow rate at the bed void fractions of 0.69 and 0.41. A possible explanation may be that the antifoaming agent increased the mass transfer resistance in the liquid, since surface-active compounds have the tendency to accumulate at the gas–liquid interface. That effect is well documented in many systems [8]. On the other hand, it was observed that average xylene mineralization to CO_2 was somewhat favored with increasing the liquid mass flow rate for all void fractions where the analysis was performed.

Table 3 shows that *o*-xylene was preferentially removed, followed by *m*-xylene and *p*-xylene. The biodegradability of all isomers was favored with increased liquid mass flow rate when bed void fraction was 0.8; for lower bed void fractions, liquid mass flow rate seemed to have no effect. Additionally, the reduction of void fraction decreases the individual isomer removal efficiency in the same order of its biodegradability. In contrast, in a conventional biofilter Ortiz et al. [11] obtained complete removal of *m*- and *p*-xylene, and 85% removal of *o*-xylene. Also using a conventional biofilter, Jorio et al. [12] report xylene biodegradation in the order of $m > p > o$. However, of the three isomers, the *o*-xylene has the smallest partition coefficient in water [13] (0.200 for *o*-xylene; 0.304 for *p*-xylene; and 0.304 for *m*-xylene, at 25 °C) and thus is the most soluble. In a biotrickling filter, where the recirculating liquid is mainly water, it is reasonable to expect that the more soluble isomer is more available to the biofilm.

Xylene isomers partition coefficients in the mineral medium were determined at 25 °C (0.500 for *o*-xylene; 0.849 for *p*-xylene, and 0.907 for *m*-xylene), and were an average of 3.2 times larger than those in water. These values indicate that either in water or in the mineral medium the solubility was in the order $o > p > m$, not considering the effect of biomass. When these results are compared with those reported elsewhere [11,14,15], there does not seem to be a consistent pattern between solubility and isomer removal selectivity. It is possible that removal selectivity is more dependent on the microorganism consortium metabolic regulation than on any other factor. For example selectivity in the liquid used to inoculate the TBAB was in the order $m > o > p$, while the same experiment performed with biomass extracted from the TBAB the selectivity was $o > m > p$.

4. Conclusions

The effects of the superficial liquid mass flow rate and the bed void fraction on the hydrodynamic and biological behavior were studied in a xylene-removing TBAB. It was found that gas–liquid pressure drop per unit length increased with the liquid mass flow rate and with decreasing bed void fraction. The addition of an antifoaming agent to the liquid phase strongly decreases pressure drop.

Dynamic liquid hold-up increased more or less proportionally with the liquid mass flow rate, reaching values as high as 0.28 at 14.1 kg/m^2 s liquid rate. At this liquid rate, when bed void fraction was reduced from 0.95 to 0.69, dynamic liquid hold-up increased from 0.18 to 0.28, and then decreased to 0.24 for a bed void fraction of 0.41. The same pattern was observed for the total liquid hold-up, the mean liquid

residence time, and wetting efficiency, although with different values for each parameter.

The TBAB showed increasing stagnant regions, channeling and internal recirculation as the bed void fraction diminished. It was also evident that the liquid flow in the TBAB deviates from plug flow.

The best TBAB performance was obtained at the bed void fraction of 0.80, where increasing the liquid mass flow rate increased xylene removal to a maximum elimination capacity of 30 g/m^3 h at 14.1 kg/m^2 s. At the bed void fractions of 0.69 and 0.41, the elimination capacity was insensitive to liquid mass flow rate. Xylene elimination capacity was reduced from 30 to 8 g/m^3 h as bed void fraction decreased from 0.8 to 0.41 at a liquid rate of 14.1 kg/m^2 s. Xylene isomers were preferentially removed in the order: *ortho* > *meta* > *para*.

From our point of view, further work should be focussed on obtaining more data and on developing correlations specific for the hydrodynamic parameters in TBAB. Attempts were made, with little success, to fit the pressure drop and liquid hold-up data to existing correlations developed for chemical trickle-bed reactors. There is a need for better estimations of the wetting efficiency, since the available equations refer to beds with an even void fraction distribution. Also, the development of methods to estimate specific gas–liquid and liquid–biofilm contact area are necessary. A better understanding of TBAB hydrodynamics may provide a better estimation of mass transfer coefficients, which would in turn allow a more rational design.

Acknowledgements

The authors wish to express their appreciation to CONACyT for the financial support provided (400200-5-34146-U and Semarnat 2002-C01-0120) and for Ms. Trejo's scholarship. The authors also thank Mr. Sergio Hernandez for the technical support provided.

References

[1] R. Lobo, S. Revah, T. Viveros, An analysis of a trickle-bed bioreactor: Carbon disulfide removal, Biotechnol. Bioeng. 63 (1999) 98–109.
[2] H. Cox, M. Deshusses, Trickling biofilters for air pollution control, in: G. Bitton (Ed.), The Encyclopedia of Environmental Microbiology, vol. 2, Wiley, New York, 2002, pp. 782–795.
[3] R. Diks, S. Ottengraf, Verification studies of a simplified model for the removal of dichlomethane from waste gases using a biological trickling filter (Part II), Bioprocess. Eng. 6 (1991) 131–134.
[4] F. Pironti, D. Mizrahi, A. Acosta, M.D. González, Liquid–solid wetting factor in trickle-bed reactors: its determination by a physical method, Chem. Eng. Sci. 54 (1999) 3793–3800.
[5] A. Gianetto, V. Specchia, Trickle bed reactors: State of the art and perspectives, Chem. Eng. Sci. 47 (1992) 3197–3213.
[6] A. Hernández, Gasoline vapors control through biofiltration, M.Sc. Thesis, Universidad Autonoma Metropolitana-Iztapalapa, Mexico, 2002 (in Spanish).
[7] M.E. Acuña, F. Perez, R. Auria, S. Revah, Microbiological and kinetic aspects of a biofilter for the removal of toluene from waste gases, Biotechnol. Bioeng. 63 (1999) 175–184.
[8] T.K. Sherwood, R.L. Pigford, C.R. Wilke, Mass Transfer, McGraw-Hill, New York, 1975.
[9] C. Lu, K. Chang, Biofiltration of butyl acetate and xylene mixtures using a trickle-bed air filter, Eng. Life. Sci. 4 (2004) 131–137.
[10] J. Paca, E. Klapkova, M. Halecky, M. Maryska, K. Kinney, Biotrickling filter: Hydrodynamics, performance characteristics and biofilm changes, in: Air & Waste Management Association. 97th Annual Conference & Exhibition, Indianapolis, Indiana, 2004.
[11] I. Ortiz, S. Revah, R. Auria, Effects of packing material on the biofiltration of benzene, toluene and xylene (BTX) vapors, Environ. Technol. 24 (2003) 265–275.
[12] H. Jorio, L. Bibeau, G. Viel, M. Heitz, Effects of gas flow rate and inlet concentration on xylene vapors biofiltration performance, Chem. Eng. J. 76 (2000) 209–221.
[13] H.J. Rafson, Odor and VOC Control Handbook, Mc Graw-Hill, New York, 1998, p.2.24.
[14] J.M. Strauss, K.J. Riedel, C.A. du Plessis, Mesophilic and thermophilic BTEX substrate interactions for a toluene-acclimatized biofilter, Appl. Microbiol. Biotechnol. 64 (2004) 855–861.
[15] C.L. Chen, R.T. Taylor, Thermophilic biodegradation of BTEX by two consortia of anaerobic bacteria, Appl. Microbiol. Biotechnol. 48 (1997) 121–128.